Europe PMC Funders Group
Author Manuscript
Sci Transl Med. Author manuscript; available in PMC 2022 November 24.

Published in final edited form as:
Sci Transl Med. 2019 May 22; 11(493): . doi:10.1126/scitranslmed.aav7325.

Phagocytosis-Shielded Lentiviral Vectors Improve Liver Gene Therapy in Non Human Primates

Michela Milani[#1,2], **Andrea Annoni**[#1], **Federica Moalli**[3], **Tongyao Liu**[4], **Daniela Cesana**[1], **Andrea Calabria**[1], **Sara Bartolaccini**[1], **Mauro Biffi**[1], **Fabio Russo**[1], **Ilaria Visigalli**[1], **Andrea Raimondi**[3], **Susannah Patarroyo-White**[4], **Douglas Drager**[4], **Patrizia Cristofori**[1,5], **Eduard Ayuso**[6], **Eugenio Montini**[1], **Robert Peters**[4], **Matteo Iannacone**[3], **Alessio Cantore**[1,2,*], **Luigi Naldini**[1,2,*]

[1]San Raffaele Telethon Institute for Gene Therapy, IRCCS San Raffaele Scientific Institute, 20132 Milan, Italy

[2]Vita Salute San Raffaele University, 20132 Milan, Italy

[3]IRCCS San Raffaele Scientific Institute, 20132 Milan, Italy

[4]Bioverativ, Waltham, MA 02451 USA

[5]Glaxo Smith Kline R&D UK, Ware, SG12 0DP United Kingdom

[6]INSERM UMR1089, University of Nantes, CHU de Nantes, 44093 Nantes, France

[#] These authors contributed equally to this work.

Abstract

Liver-directed gene therapy for the coagulation disorder hemophilia showed safe and effective results in clinical trials using adeno-associated viral vectors to replace a functional coagulation factor, although some unmet needs remain. Lentiviral vectors (LV) may address some of these hurdles because of their potential for stable expression and the low prevalence of pre-existing viral immunity in humans. However, systemic LV administration to hemophilic dogs was associated to mild acute toxicity and low efficacy at the administered doses. Here, exploiting intravital microscopy and LV surface engineering we report a major role of the human phagocytosis inhibitor CD47, incorporated into LV cell membrane, in protecting LV from uptake by

[*]To whom correspondence should be addressed: cantore.alessio@hsr.it, naldini.luigi@hsr.it.
[*]These authors share senior authorship

Author contributions

M.M. and A.A. designed and performed experiments, analyzed and interpreted data and wrote the manuscript. F.M. designed and performed IV2PM experiments, analyzed data and edited the manuscript. T.L. set up and performed FIX and Abs assays, analyzed data and edited the manuscript. D.C. and A. Cal. performed IS analysis and analyzed data. S.B., M.B., F.R. performed experiments and analyzed data. I.V. set up and performed VCN assays on NHP samples. A.R. performed electron microscopy experiments. S.P.-W. and D.D. performed FIX and Abs assays. P.C. supervised I.V. research. E.A. coordinated experiments with NHP, interpreted data and edited the manuscript. E.M. supervised D.C. and A. Cal. for IS analysis and interpretation and edited the manuscript. R.P. supervised T.L. research. M.I. supervised F.M. research and edited the manuscript. L.N. and A. Can. conceived the project, supervised research, interpreted data and wrote the manuscript. L.N. provided overall coordination.

Competing interests

L.N., A.C, A.A., M.M., R.P., T.L., S.P.-W. are inventors on patent applications (Vector Production, P105283GB, P114659GB) submitted by Foundation Telethon (F.T.) and San Raffaele Scientific Institute (S.R.S.I.) or Bioverativ on LV technology related to the work presented in this manuscript. F.T. and S.R.S.I., through SR-Tiget, have established a research collaboration on liver-directed lentiviral gene therapy of hemophilia with Bioverativ.

Europe PMC Funders Author Manuscripts
Europe PMC Funders Author Manuscripts

Europe PMC Funders Author Manuscripts

Europe PMC Funders Author Manuscripts

professional phagocytes and innate immune sensing, thus favoring biodistribution to hepatocytes following systemic administration. By enforcing high CD47 surface content, we generated phagocytosis-shielded LV which, upon intravenous administration to non-human primates, showed selective liver and spleen targeting and enhanced hepatocyte gene transfer compared to parental LV, reaching supra-physiological activity of human coagulation factor IX, the protein encoded by the transgene, without signs of toxicity or clonal expansion of transduced cells.

Introduction

Liver-directed gene therapy for the treatment of the inherited coagulation disorder hemophilia is among the most successful application of gene therapy (1). Protein replacement therapy (PRT) with recombinant coagulation factor VIII or IX (FIX), whose activity are lacking in hemophilia A or B, respectively, is the standard of care. Gene therapy, however, may establish a stable tissue source of functional factor after a single administration, bypassing the lifelong requirement of frequent intravenous (i.v.) PRT infusion and potentially providing a definitive cure of the disease. Indeed, a single i.v. administration of recombinant adeno-associated virus (AAV) derived vectors delivering a functional copy of a clotting factor gene to the liver, its natural site of production, has shown safety and efficacy in patients with hemophilia and is poised to become a clinically available treatment option (2–4). However, because AAV vectors do not actively integrate into the host cell genome and the anti-AAV immune responses limit vector re-administration (1, 5), it may be difficult to apply this type of gene therapy to pediatric patients. Moreover, a sizable fraction of adult patients is immunized against AAV, thus they are either not eligible to receive AAV vector administration, due to neutralizing anti-AAV antibodies, or necessitate immune suppression for a period of time to maintain AAV-transduced hepatocytes, due to cellular immunity against AAV capsids (1, 5). On the contrary, human immunodeficiency virus (HIV)-derived lentiviral vectors (LV) integrate into the target cell chromatin and are maintained as cells divide, a potential advantage for establishing long-term expression if not associated with a significant risk of insertional mutagenesis (6, 7). Furthermore, the lower prevalence of HIV compared to AAV infection in humans (www.who.int/gho/hiv), make LV attractive gene delivery vehicles to complement the reach and broaden the scope of AAV-vector based gene therapy for liver diseases. We have developed LV that achieve stable transgene expression in the liver and reconstitute FIX activity in mouse models of hemophilia B, without detectable evidence of genotoxicity(8, 9). These outcomes are dependent on stringent targeting of expression to hepatocytes by combining transcriptional and post-transcriptional, microRNA-mediated regulation (10). However, systemic LV administration to dogs was associated to a mild acute toxicity, and efficacy was low at the administered LV doses (9).These limitations might reflect poor biodistribution of i.v. administered LV to hepatocytes, possibly due to fast clearance from the circulation by hepatic and splenic professional phagocytes, which in turn trigger innate immune activation upon sensing the taken up viral particles. For these reasons we set out to investigate LV biodistriution to different liver cell types after i.v. administration of escalating LV doses and counteract their capture by professional phagocytes exploiting a natural inhibitor, CD47. By this strategy we generated phagocytosis-shielded LV with higher efficiency of hepatocyte gene transfer and reduced activation of acute inflammatory

Europe PMC Funders Author Manuscripts

Europe PMC Funders Author Manuscripts

response, following i.v. administration, and evaluated their safety and efficacy in non-human primates (NHP).

Results

Professional phagocytes in the liver uptake most i.v. administered LV

We first evaluated the correlation between the administered dose of LV bearing a hepatocyte-specific FIX expression cassette (LV-FIX) (8) and transgene expression in C57BL/6 adult mice (n=48). The previously described hepatocyte-specific expression cassette contains an engineered hepatocyte-specific promoter (Enhanced Transthyretin) and target sequences for the hematopoietic-lineage specific microRNA 142, abrogating off-target transgene expression in antigen-presenting cells (APC) in the liver and spleen (11). We observed a non-linear dose response and a rapid increase in FIX output above a threshold dose, achieving approximately 1 μg/mL (corresponding to 20% of normal) at $3x10^{10}$ transducing units (TU)/kg LV dose (Fig. 1A). Professional phagocytes in the liver and spleen provide a major clearance mechanism for blood-born particles, including viral vectors (12, 13). We thus investigated the biodistribution of intravenously administered LV to the spleen and liver cell subpopulations. We administered 1, 2 or $4x10^{10}$ TU/kg (n=10 *per* dose) of LV expressing GFP to C57BL/6 adult mice and measured transgene expression and vector copies *per* diploid genome (vector copy number, VCN) 2 months thereafter. Whereas both the percentage of GFP-positive hepatocytes and VCN in total liver DNA nearly doubled from 1 to $2x10^{10}$ TU/kg, there was a disproportionately higher increase in GFP-positive hepatocytes when further doubling the vector dose (Fig. 1B), in line with the non-linear dose-response observed for LV-FIX. We then separated cellular fractions enriched in hepatocytes (parenchymal cells, PC) from non-parenchymal cells (nPC) in freshly dissociated livers. We further purified hepatocytes (Hep) from the PC fraction, and liver sinusoidal endothelial cells (LSEC), Kupffer cells (KC) and plasmacytoid dendritic cells (pDC) from total nPC by FACS (Fig. S1) and measured the VCN in these subpopulations. We observed 9-28 fold highervery high VCN in KC than PC at all tested doses, reaching 27. This high VCN in nPC and KC plateaued at increasing LV doses (Fig. 1C). It is reported that the liver comprises approximately 70% PC and 30%nPC, of which 50% are LSEC (15% of total), 20% are KC (6% of total) and the remaining 30% are biliary ducts cells, hepatic stellate cells, and other cells (14). We thus calculated the relative contribution to the total liver vector content of each sub-population, considering their reported abundance, and estimated that only about 30% of the liver LV DNA is found in PC at low doses, while it becomes >50% at the highest dose. Conversely, almost 70% of the LV DNA is found in nPC at the low doses and about 40% at the highest dose (Fig. S2A). There was a linear correlation between the VCN measured in total liver samples at each LV dose and that calculated summing up the contributions of each subpopulation (Fig. S2B-D). Whereas the best-fit correlation between the percentage of GFP-positive hepatocytes and total liver VCN was exponential, a perfectly linear correlation was found between GFP-positive hepatocytes and the VCN in PC (Fig. S2E,F). These data indicate that the VCN measured in total liver does not reflect the percentage of hepatocyte transduction, due to the different distribution of LV DNA observed within the liver cell subpopulations at different LV doses. Moreover, the results suggest that as the LV input reaches a threshold dose, LV uptake by KC is saturated

Europe PMC Funders Author Manuscripts

Europe PMC Funders Author Manuscripts

and more LV are available to transduce hepatocytes, thus giving rise to a non-linear dose response for hepatocyte gene transfer and transgene expression.

Recognition of human CD47 on LV particles inhibits phagocytosis and increases hepatocyte gene transfer

Phagocytosis is physiologically inhibited by CD47, a ubiquitously expressed species-specific ligand of signal regulatory protein α (SIRP-α) receptor expressed by professional phagocytes (15). Human CD47 is incorporated into LV when they bud from producer cells. It has been shown that SIRP-α of non-obese diabetic (NOD) mice has high affinity for human CD47 (16). We thus compared the outcome of LV-FIX administration to NOD mice and C57BL/6 *F9* knock out mice, a mouse model of hemophilia B. We observed a significantly longer half-life of LV particles in the first hour upon bolus i.v. injection (p=0.0001) and >10-fold higher FIX expression in the blood (p=0.0046) in NOD compared to C57BL/6 mice (Fig. 1D,E). Consistently with the increased FIX output, we found 4-fold higher LV VCN in sorted hepatocytes and 30- and 5-fold lower VCN in KC and spleen, respectively, in NOD vs. C57BL/6 mice (Fig. 1F). LV copies were also >10-fold lower in NOD pDC, which are known sensors of viral nucleic acid and were reported to release type-I IFN after exposure to LV particles (17). We confirmed a strong correlation between the VCN in sorted hepatocytes and FIX expression (Fig. S2G). Based on the VCN in the liver cell subpopulations, we estimated that only about 5% of the liver LV DNA was in sorted hepatocytes in C57BL/6 mice, while it was about 50% in NOD mice (Fig. S2H). Despite the higher VCN in sorted hepatocytes found in NOD compared to C57BL/6 mice, the VCN measured in total liver samples was lower in the former compared to the latter strain (Fig. S2I), further confirming that VCN in bulk liver does not reflect the extent of transduction of hepatocytes. Indeed, when we calculated the expected liver VCN based on the relative contribution of the VCN measured in sorted hepatocytes and KC (from Fig. 1F) we obtained a higher total liver VCN in C57BL/6 compared to NOD mice (Fig. S2I). To confirm the role of human CD47 in the observed outcome, we repeated the experiment with LV produced by cells in which we disrupted the *CD47* gene by CRISPR/Cas9 (CD47-free LV, Fig. 1G-I, Fig. S2J and Fig. S3). The inter-strain differences in LV half-life, transgene expression, and biodistribution among liver cell types, observed when we administered LV, were almost completely abrogated when we administered CD47-free LV, at both lower and higher doses, indicating that the interaction between the NOD SIRP-α and the human CD47 molecule on LV particles was primarily responsible for the differences observed between the two strains. These findings underline a major role of CD47 in inhibiting LV uptake by phagocytes and innate immune sensors, substantially affecting LV in vivo biodistribution.

CD47 overexpression in producer cells protects LV from uptake by human macrophages

Because the density of CD47 molecules is differentially regulated among distinct cell types and can determine their susceptibility to phagocytosis (18–21), we exposed a human macrophage cell line or human primary macrophages to LV and found a higher content of LV genome than in 293T reference cells, suggesting that LV is actively phagocytized by these cells and that the amount of CD47 incorporated in the LV particles might be rate-limiting for inhibiting phagocytosis by human cells (Fig. 2A,B). Note that the high content of LV genome did not correspond to high transgene expression, consistently with the

Europe PMC Funders Author Manuscripts

Europe PMC Funders Author Manuscripts

reported post-entry restriction of LV transduction in human mature macrophages (22, 23). We thus engineered both LV stable producer cell lines previously reported in (24) and 293T cells used for LV production by transient transfection, to overexpress CD47. To this end, we transduced these cells with CD47-expressing self-inactivating γ-Retroviral Vector (SIN RV), which cannot be cross-packaged by LV (25). We achieved stable 10-30 fold overexpression of the CD47 protein on the cell surface of both 293T and LV producer cell lines (CD47hi cells; Fig. S4A-E). LV produced by CD47hi cells had comparable titer and infectivity on reference 293T cells as vectors produced by the parental cells (Fig. S4F-K) and showed significantly increased ($p<0.0001$) immunostaining for CD47 by electron microscopy (Fig. 2C,D). The amount of CD47 on the LV surface did not affect the presence of the envelope protein, vesicular stomatitis virus protein G (VSV.G), consistently with unaltered infectivity of CD47hi LV (Fig. 2E). When matched input of CD47hi and control LV were incubated with a macrophage cell line or primary human macrophages, we found a significantly reduced uptake of CD47hi LV ($p=0.0303$), which approached reached the basal level observed in the reference 293T cells (see Fig. 2A,B). Conversely, we found a significantly higher uptake of CD47-free than control LV ($p=0.0083$) by human macrophages (Fig. 2F). These data indicate that modulating the quantity of CD47 on LV particles affect their uptake by human macrophages.

CD47hi LV show reduced susceptibility to phagocytosis and innate immune activation in NOD mice

We then evaluated whether CD47 amount affected LV biodistribution in vivo, using the NOD mouse strain, which recognizes the human CD47. The half-life in the blood was significantly higher ($p=0.0005$) for CD47hi than control LV (Fig. 2G), with a dose-dependent change in biodistribution. At lower vector doses, KC uptake of control LV was significantly higher ($p=0.0157$) than uptake of CD47hi LV (Fig. 2H). At higher vector doses, KC uptake was reduced for both vector types, compared to the lower vector doses (Fig. 2I, S5A). These data suggest that the density of CD47 on the control LV surface is limiting and inhibits phagocytosis by liver KC and other APC only at high LV doses, when the total particle input may act by bulk action (non-particle autonomous), whereas CD47hi LV are consistently protected at the individual particle level even at low input. There was no difference in hepatocyte transduction or FIX expression between CD47hi LV and control LV in these experimental settings (Fig 2H-J). Differential surface display of CD47 impacted the acute cytokine and chemokine release, following i.v. LV administration. Specifically, macrophage inflammatory protein 1 (MIP-1α, $p=0.0363$), MIP-1β($p<0.0001$), MCP1 ($p=0.0007$), CXCL1 ($p=0.0002$) and granulocyte-colony stimulating factor (G-CSF, $p<0.0001$) significantly increased in LV-treated compared to untreated NOD mice, 3 hours after LV administration and then returned to baseline 2-7 days post LV depending on the cytokine, whereas their serum concentration was not different in CD47hi-LV treated compared to untreated NOD mice (Fig. 2K-O and Fig. S5B-F). Conversely, administration of CD47-free LV to NOD mice triggered the strongest increase in these macrophage-related cytokines (Fig. 2K-O). These data are in line with the observed modulation of APC uptake by the CD47 content of the LV particles.

Europe PMC Funders Author Manuscripts

Europe PMC Funders Author Manuscripts

Intravital imaging shows that CD47 regulates the rate and extent of LV phagocytosis by KC

To investigate the kinetics of LV phagocytosis in the liver in real time upon i.v. administration, we performed intravital two-photon microscopy (IV2PM). To visualize LV, we produced them in control 293T, CD47hi 293T or CD47-negative 293T cells expressing GFP fused to the membrane-targeting domain of $pp60^{Src}$, a chimeric protein previously shown to be effectively incorporated in the budding HIV envelope (26). LV uptake was recorded live in the surgically exposed liver of anesthetized mice (27). We observed that administration of GFP-labeled LV in C57BL/6 mice resulted in rapid and widespread uptake by KC (visualized by red fluorescent anti-F4/80 antibody infusion prior to LV administration (28)), which became 90% LV-positive in the examined fields within 4-8 minutes upon administration (Fig. 3 and Movie S1). By contrast, we observed that administration of the same LV into NOD mice reached 90% LV-positive KC only after 15-28 minutes post LV. When CD47hi LV were administered to NOD mice only 12-52 % of KC became LV-positive at the end of recording (38 minutes post LV). Note that the GFP signal is lost once LV envelope fuses with endosome membrane and the LV core escapes into the cytoplasm. According to this design, we could follow LV accumulation in KC endo-phagosomes (yellow signal), but not hepatocyte transduction, because of overall lower LV entry *per* cell. The CD47-free LV uptake by KC observed in NOD mice appeared overlapping with that observed in control LV injected in C57BL/6 mice, reaching 90% LV-positive KC 6 minutes post LV. These data provide visual evidence that the recognition and content of CD47 on the LV surface impacts timing and extent of LV uptake by KC and, together with the results shown above, indicate a major role of this molecule in shielding LV from phagocytosis in vivo.

Intravenous administration of phagocytosis-shielded LV to NHP is safe and well tolerated

Because the sequence homology of SIRP-α and CD47 between NHP and humans is 94% and 99%, respectively, whereas the murine SIRP-α and CD47 are only 70-75% homologous to the human genes, we predicted that the protection afforded by CD47 to LV may be even more effective in NHP, which represent the closest model to humans. We chose *Macaca nemestrina* as recipient, because of the lower restriction to HIV infection compared to other NHP species (29, 30). We produced large scale batches of control or CD47hi LV using the previously described major histocompatibility complex (MHC)-free 293T cells (24), purified and qualified for potency, purity, and sterility according to the protocol and specifications used for clinical-grade LV (Table S1 and Fig. S6A). We administered these LV *via* a peripheral vein to 6 NHP at the target dose of $7.5x10^9$ TU/kg (3 for each LV version). The infusion was well tolerated, with only a minor elevation of aspartate aminotransferase one day after administration (2-fold the pre-administration value), and with serum alanine aminotransferases and body temperature remaining within the mean ± 3 standard deviations (SD) of pre-treatment values (Fig. 4A-C; Tables S2-8). We observed a transient self-limiting leukopenia, mostly noted in lymphocytes, one day after LV administration, which might be explained by migration of these cells into the liver (Fig. 4D,E). We measured a panel of 23 cytokines in the serum of treated NHP before and after LV administration and observed a transient increase in IL-2, IL-1 receptor antagonist (RA), IL-18, IL-10 and the macrophage-related cytokines MIP-1α, MIP-1β and MCP-1, compared to the vehicle-treated animal, suggesting mild self-limiting inflammation (Fig. S6B-H). In line with the data shown above

Europe PMC Funders Author Manuscripts

Europe PMC Funders Author Manuscripts

in NOD mice, we observed a milder rise in MIP-1α, MIP-1β and MCP-1 in CD47hi-LV compared to LV-treated NHP and the concentrations of these chemokines in CD47hi-LV treated animals were nearly overlapping with those of the vehicle-treated subject (Fig. S6B-H). Overall, these data show that in vivo administration of LV to NHP is safe and well tolerated and suggest reduced activation of the innate immune system by CD47hi LV.

Intravenous administration of LV to NHP results in robust hepatocyte gene transfer further increased by CD47hi LV

We measured human-specific FIX antigen and activity in the plasma of treated NHP and found an average of 1 μg/mL and 1 U/mL (corresponding to 20% and 100% of normal, respectively) in LV-treated animals, which was stable for 90 days post LV, when the study was terminated (Fig. 4F,G). Instead FIX antigen and activity were 2.9 μg/mL and 2.42 U/mL (corresponding to 58% and 242% of normal, respectively) on average in CD47hi-LV treated animals, nearly 3-fold higher than those of LV-treated animals (p=0.0002 Fig. 4F; p<0.0001 Fig. 4G), in the first month post LV. Note that FIX activity was 4-5 fold higher than antigen, as expected by the use of the hyper-functional FIX Padua variant (8, 31). After the first month of follow-up, the 3 NHP expressing higher FIX developed anti-human FIX Abs at increasing titer with increasing FIX level (Fig. 4H,I), in line with other studies administering high doses of recombinant human FIX or vectors expressing human FIX to NHP (32, 33). The emergence of low-titer non-neutralizing anti FIX Abs in CD47hi-LV2 and 3 was associated with the formation of detectable circulating immune complexes (Fig. 4J), which likely caused a concomitant over-estimation of human-specific FIX antigen and activity by the immune capture assays towards the end of the study (see Fig. 4F,G). Instead, the higher titer, neutralizing anti-FIX Abs developed by CD47hi-LV1 caused human FIX antigen and activity to become undetectable (Fig 4I). By measuring p24 in the serum of treated NHP, we observed almost overlapping clearance of the two LV versions, with a 4-log decrease in serum p24 the day after LV administration and becoming undetectable 1 week after LV administration (Fig. S7A). The serum concentration of C3a increased above the mean ± 3SD of pre-treatment values shortly after LV administration suggesting that part of circulating LV particles may be lysed by the complement system (Fig. S7B). As expected, all the animals developed anti-VSV.G Abs (Fig. S7C). After necropsy, we measured LV DNA in liver, spleen and major organs of treated animals. and We found between 0.5 and 1.8 LV VCN in the liver, accounting for 80-90% of all the retrieved LV DNA, showing selective targeting of the liver by LV in NHP, with almost a 3-log difference in VCN measured in the liver and the highest VCN measured in the other organs (Fig. 5A). In line with the mouse data, the measured FIX output was higher but not the total liver VCN in CD47hi-LV treated compared to LV-treated NHP., These findings likely reflecting reflect a different vector distribution between liver cell subpopulations, favoring hepatocyte transduction and decreasing KC uptake for CD47hi-LV. Increased hepatocyte transduction in CD47hi-LV treated NHP was further indicated by measuring LV RNA expression, which is selectively targeted to hepatocytes, in liver samples and performing RNA *in situ* hybridization (ISH) on liver slices with a probe targeting the woodchuck hepatitis virus post-transcriptional regulatory element (WPRE) present on the transgene RNA. We found higher LV RNA content (p=0.0358) and more LV-expressing cells (p<0.0001) in the livers of CD47hi-LV than LV-treated NHP, except in CD47hi-LV1, who showed hardly any

Europe PMC Funders Author Manuscripts

Europe PMC Funders Author Manuscripts

LV RNA and very few LV-expressing cells, suggesting delayed clearance of transduced hepatocytes accompanying the development of neutralizing anti-human FIX Abs (Fig. 5B-D). We estimated the difference in LV VCN of KC compared to hepatocytes of CD47hi-LV and LV treated NHP based on a mathematical model built on experimental data obtained in mice (Fig. S7D,E). Pathology analysis of liver, spleen and major organs was performed by 2 independent veterinary pathologists at the end of the study in all NHP, including the vehicle-treated control and no macroscopic or microscopic lesions were reported, except for splenic follicular hyperplasia and minimal liver inflammatory foci found in vector-treated NHP, which could not be conclusively attributed to vector treatment because of the single control animal analyzed and whose features were considered within the range of normal for NHP. Blood hematology and clinical biochemistry parameters were within the range of pre-treatment values in the follow-up of vector administration, except for minor fluctuations (see Table S2-8).

Quantitative high-throughput vector integration site (IS) analysis performed at the end of the study on genomic DNA from multiple liver and one spleen sample from all NHP showed high diversity, with thousands of distinct IS contributing by few occurrences to the total (Fig. 5E, Fig. S8A, Table S9). There were no dominant clones in the liver or spleen of all NHP analyzed, and >93% IS were represented by 1 to 4 genomes, while the remaining IS were represented by a maximum abundance of 32 genomes (Fig. 5F, Fig. S8B). The frequency of IS mapping near or within cancer genes, defined by the oncogenes and tumor suppressor genes listed in Uniprot for both human and murine annotations, was approximately 2% on average, similar to the percentage of cancer genes in the whole genome and did not show enrichment even in the few IS with an abundance of >4 genomes (Table S10). The genomic distribution of IS across the genome showed the appearance of few hot spots (common IS; Table S11), which, with few exceptions, clustered in regions syntenic to human genomic regions known to be frequently targeted by LV insertions in human hematopoietic cells as the result of an intrinsic integration bias of the parental virus not associated with genotoxicity (34–36). IS were more enriched in liver vs. spleen ($p<0.0001$) when comparing the CD47hi vs. control LV group (see Table S9), likely reflecting the CD47 action.

Overall, we describe efficient liver gene transfer in NHP, which is further and substantially increased by CD47hi LV, likely due to skewed vector biodistribution within the liver, favoring transduction of hepatocytes at the expense of KC, and leading to human specific FIX activity in the plasma up to supra-physiological, without molecular evidence of clonal expansion of transduced cells or enrichment of LV IS at cancer genes.

Discussion

Here we show tolerability, selectivity and efficiency of liver gene transfer following systemic i.v. LV administration to NHP. We observed a more favorable LV dose-response for FIX expression in NHP, than in dogs and mice, which required a 4-fold higher dose to reach the same FIX output. This favorable outcome may be due, at least in part, to better recognition of the human CD47 present on LV by the NHP SIRP-α receptor as compared to its murine or canine counterpart. In addition, HIV has evolved mechanisms to evade intracellular sensing and innate immune triggering in humans (37), which may further

Europe PMC Funders Author Manuscripts

Europe PMC Funders Author Manuscripts

explain the limited acute reaction to i.v. LV administration observed in *Macaca nemestrina* in our study. The preferential gene transfer to the liver and spleen by VSV-G pseudotyped LV, despite systemic administration and the well-known VSV-G pantropism, may be due to the abundant blood supply to these filter organs, the facilitated access to perisinusoidal space by the discontinuous microvascular endothelium and the engagement of low-density lipoprotein (LDL) receptors on hepatocytes by VSV-G on vector particles (38), mimicking LDL uptake. This LV biodistribution, combined with tailored choices of transcriptional and post-transcriptional regulation (39, 40), provides a platform for stringently targeting transgene expression to specific cell types within the liver or spleen, as shown here for hepatocytes.

The major role of the producer cell-derived CD47 molecule in modulating LV biodistribution among liver and spleen cell types shown here is consistent with previous observations that incorporation of CD47 increases the half-life and decreases phagocytosis of i.v. administered nanoparticles and LV particles in a SIRP-α dependent manner (20, 41). Here we extend these findings as we compared mice permissive or refractory to human CD47 signaling, and LV with or without CD47, and show that decreased clearance by professional phagocytes favors LV transduction of hepatocytes and alleviates the innate immune response to systemic administration. Furthermore, intravital imaging of the liver during LV administration provided direct evidence of the rapid scavenging of vector particles from the sinusoids by mouse KC and the rate-limiting function of CD47 on the vector surface in modulating this clearance mechanism. LV with high surface content of CD47, besides being more resistant to phagocytosis, were also less prone to innate immune sensing by APC and showed improved efficiency of gene transfer to hepatocytes in NHP, compared to LV with basal content of CD47. Such increase in hepatocyte transduction and FIX output by CD47hi LV was not observed in NOD mice. The difference between mice and NHP may be due, at least in part, to the different rate of i.v. administration, which was performed by bolus injection in mice and by slow infusion (10 mL/kg/h) in NHP. In the former setting, a peak of LV blood concentration at the beginning of infusion may have allowed CD47 to act by total mass action (non-particle autonomous) on professional phagocytes, thus masking the benefit provided by increasing the CD47 density *per* LV particle, which might instead be more relevant at lower LV blood concentrations, as upon the slow LV infusion performed in NHP. This explanation is also consistent with our interpretation of the different extent of KC uptake and its modulation by CD47 at high vs. low input vector doses in NOD mice. Different liver histological features, such as the size of LSEC fenestrations, may also contribute to the different LV dose-response observed for hepatocyte gene transfer in different animal models (42). Note, however, that CD47hi LV did not show delayed clearance from the circulation as compared to control LV in NHP, suggesting that additional complement-mediated mechanisms might contribute to clear non-phagocytized CD47hi LV from the circulation, by direct lysis or opsonization of complement-bound particles that have lost transduction capacity. In support of this hypothesis, we observed a higher peak of complement activation in CD47hi-LV than LV-treated NHP.

Anti-human FIX immune responses were observed in this as well as previous gene therapy studies performed in NHP with different vectors (33, 43) and may raise concerns for clinical

Europe PMC Funders Author Manuscripts

Europe PMC Funders Author Manuscripts

translation. The association of immune response with high human FIX concentration in the blood and the delayed time of onset suggest that these responses may be mediated by cross-presentation in MHC class I and II of FIX antigen taken up from the circulation by APC, and thus were not fully prevented by shielding LV from phagocytosis at the time of administration. Of note, such immune responses may not necessarily imply a risk when translating the treatment in previously exposed Abs-negative patients.

Whereas genome-wide LV integration necessarily implies a concern for delayed oncogenesis, our findings show no signs of expansion of LV-transduced hepatocytes nor of liver tumors in NHP, albeit within the inherent limitations of number of treated subjects and length of observation. Indeed, LV IS analysis in NHP liver and spleen showed diverse composition with nearly all unique IS being represented by 1-4 genomes, indicating that no clonal expansions have occurred and consistently with the low to null proliferation rate expected for most liver cells in the treated NHP. Moreover, at the best of our knowledge, no evidence of insertional oncogenesis has been reported until now in hundreds of patients treated by LV-transduced hematopoietic stem cells (HSC) or T cells in several clinical trials, with a follow-up of >10 years for the earliest treated patients (1, 6). These findings are reassuring, given the sensitivity of HSC to oncogenic transformation, which is likely to be higher than hepatocytes, and support the claim that LV design, IS selection and polyclonal reconstitution all contribute to alleviate such risk.

The main limitations of this work are the small sample size of the NHP study, due to feasibility and ethical reasons, a relatively short window of observation of LV-treated NHP, which cannot exclude long-term adverse effects due to insertional mutagenesis, and the single vector dose evaluated when comparing CD47hi- and parental LV in NHP, which calls for additional preclinical studies at lowered vector doses to further evaluate the safety, efficacy and immunogenicity of in vivo gene therapy with CD47hi LV. Overall, the enhanced therapeutic index of phagocytosis-shielded CD47hi LV should allow reducing the effective LV dose, thus easing manufacturing demand, alleviating concerns for any residual dose-dependent LV toxicity, and paving the way to future clinical testing with the aim to broaden applicability of liver gene therapy to more hemophilia patients and, possibly, other diseases.

Materials and Methods

Study design

Sample size in experiments with mice was choosen according to previous experience with experimental models and assays. Mouse studies were designed to evaluate susceptibility of LV to phagocytosis after i.v. administration. LV-derived transgene expression was measured in the plasma of treated animals and LV transduction of different cell types was determined at end-point. NHP study was designed to evaluate acute toxicity, transduction efficiency and biodistribution of i.v. administered LV, by measuring transgene expression in the plasma, blood chemistry, histological and molecular analyses. Sample size in the NHP study was limited by ethical and feasibility reasons. No sample or animal was excluded from the analyses. Mice and NHP were randomly assigned to each experimental group. Investigators were not blinded.

Europe PMC Funders Author Manuscripts

Europe PMC Funders Author Manuscripts

Vector production

Large-scale purified LV batches used for the NHP study were produced by MolMed S.p.A., as previously described (9), and formulated in PBS 5% dimethyl sulfoxide (DMSO). Results of selected quality control assays performed on these batches are reported in Table S1. A sterile "vehicle" solution (PBS 5% DMSO) was prepared in parallel. Lab-grade VSV.G-pseudotyped third-generation self-inactivating (SIN) LV were produced by calcium phosphate transient transfection into 293T cells, or by LV stable producer cell lines (24). 293T cells were transfected with a solution containing a mix of the selected LV genome transfer plasmid, the packaging plasmids pMDLg/pRRE and pCMV.REV, pMD2.G and pAdvantage, as previously described (9). Medium was changed 14-16 hours after transfection and supernatant was collected 30 hours after medium change. Alternatively, LV production was induced when LV producer cells were in a sub-confluent state, by replacing the culture medium with medium containing doxycycline (Sigma) 1 μg/mL and supernatant was collected 3 days after induction. LV-containing supernatants were sterilized through a 0.22 μm filter (Millipore) and, when needed, transferred into sterile poliallomer tubes (Beckman) and centrifuged at 20,000 g for 120 min at 20° C (Beckman Optima XL-100K Ultracentrifuge). LV pellet was dissolved in the appropriate volume of PBS to allow 500-1000X concentration. VSV.G-pseudotyped SIN RV were produced by calcium phosphate transient transfection into 293T cells. 293T cells were transfected with pRT43.3.PGK.CD47, the packaging plasmid pCMV-Gag/Pol (Moloney Leukemia Virus) and pMD2.G, as described (44). Medium was changed 14-16 hours after transfection and RV-containing supernatant collected 30 hours after medium change and concentrated 1000X by ultracentrifugation as above.

Mice experiments

Founder C57BL/6 *F9* knock out mice were originally obtained from the laboratory of Dr. Inder Verma at the Salk Institute (45). NOD and wild-type C57BL/6 mice were purchased by Charles River. All mice were maintained in specific pathogen-free conditions. Vector administration was carried out in adult (7-10 week old) mice by tail-vein injection. Mice were bled from the retro-orbital plexus using capillary tubes and blood was collected into 0.38% sodium citrate buffer, pH 7.4. Mice were deeply anesthetized with tribromoethanol (Avertin) and euthanized by CO_2 inhalation at the scheduled times. All animal procedures were performed according to protocols approved by the Institutional Animal Care and Use Committee.

Intravital imaging

C57BL/6 or NOD mice were surgically prepared for liver IV2PM as described (28). Mice were i.v. injected with PE-conjugated anti-F4/80 Ab (clone BM8, Biolegend) 20 min before imaging. GFP-labeled LV, CD47hi or CD47-free LV were i.v. injected 2 min after the start of video recording. Images (TriMScope II) were obtained with a Nikon Ti-U fluorescence inverted microscope and a 25x objective (NA 0.95). For four-dimensional analysis, 8–12 z-stacks (spacing 4 μm) of 300- to 400-μm^2 xy-sections were acquired every 20 seconds for 40 min. Liver sinusoids were visualized by injecting i.v. non-targeted Quantum Dots 655

Europe PMC Funders Author Manuscripts

Europe PMC Funders Author Manuscripts

(Invitrogen) immediately prior to imaging. Sequences of image stacks were transformed into volume-rendered four-dimensional videos using Imaris software (Bitplane).

NHP study

Seven adults (3-5 kg body weight) male *Macaca Nemestrina* were purchased by Bioprim (Baziège, France). Macaques were housed in an enriched environment with access to toys, fresh fruits, and vegetables at the Boisbonne Center (Nantes, France), under protocol APAFIS#4302-2015122314563838 that was approved by the Institutional Animal Care and Use Committee of the Pays De Loire. For LV administration, animals were anesthetized with Demetomidine (Domitor) 30 μg/kg and Ketamine 7 mg/kg and maintained under gas anesthesia, 1-2% Isoflurane (Vetflurane). The LV-containing solution or vehicle solution (PBS 5% DMSO) was administered using a syringe with controlled flow rate fixed at 10 mL/kg/hour via a catheter in the saphenous vein for an approximate time of 2 hours. The administered LV dose was verified by sampling and titering the dosing solution at the end of infusion. Whereas 5 out of 6 animals received the target dose, between 6.9 and $7.7x10^9$ TU/kg, one animal (CD47hi-LV2) received a higher dose of $1.0x10^{10}$ TU/kg CD47hi LV, due to a mistake in pooling LV aliquots of different volume. Note, however, that this animal showed the lowest transgene expression among its group, thus suggesting that the slightly higher administered dose was not instrumental in driving the outcome of higher transgene expression for the CD47hi LV group. An anti-inflammatory and antihistamine pre-medication regimen was administered: dexamethasone (Dexadreson, 0.3 mg/kg) i.v. 24 hours before LV and just before LV and Dexchlorpheniramine (Polaramine, 4 mg/kg) i.v. 30 minutes before LV. Blood samples were taken at different time points from the femoral vein upon anesthesia with 10 mg/kg ketamine (Imalgene) intramuscularly. For hematology, 1 mL of total blood samples was collected on EDTA-coated tubes. For clinical biochemistry, 2 mL of total blood samples was collected on heparin-coated tubes and for hemostasis, 1.8 mL of total blood was collected in citrate-coated tubes. Blood tests were performed on fresh samples at the Veterinary School of Nantes (LDHvet, Oniris). Biochemistry parameters were analyzed by automatons and analyzers based on spectrometry, reflectometry, potentiometry and enzyme immunoassays. Hemostasis was analyzed by a hemostasis analyzer based on electro-mechanical clot detection (viscosity-based detection system). Tissue samples were collected following euthanasia, performed by overdose pentobarbital sodium (Dolethal) i.v. injection.

FIX assays

The concentration of human FIX was determined in mouse plasma by an enzyme-linked immunosorbent assay (ELISA) specific for human FIX antigen (Asserachrom IX:Ag, Stago) following manufacturer's instructions. Absorbance of each sample was determined spectrophotometrically, using a Multiskan GO microplate reader (Thermo Fisher Scientific) and normalized to antigen standard curves. The concentration of human FIX was determined in NHP plasma by an ELISA specific for human FIX antigen (Haematologic Technologies, AHIX-5041). Human FIX activity was quantified in NHP plasma by a modified FIX chromogenic assay, human FIX in plasma samples was first captured by a human FIX specific Ab immobilized onto a 96-well plate (Haematologic Technologies, AHIX-5041) then chromogenic activity of human FIX was measured using Hyphen Biophen Factor IX

Europe PMC Funders Author Manuscripts

Europe PMC Funders Author Manuscripts

kit (Aniara Corp., 221806-RUO) following manufacturer's instructions. Standard curves were obtained by diluting recombinant human FIX (BENEFIX, Pfizer) into untreated NHP plasma. Total anti-human FIX Abs were quantified in heat-inactivated NHP serum by ELISA, coating recombinant human FIX (BENEFIX, Pfizer) and developing with a HRP-conjugated mouse anti-monkey IgG Ab (Southern Biotech 1:8,000). Anti-human FIX / human FIX complexes were quantified in NHP serum by ELISA, coating with a human-FIX specific Ab (Haematologic Technologies, AHIX-5041) and developing with a HRP-conjugated mouse anti-monkey IgG Ab (Southern Biotech 1:8,000). Absorbance of each sample was determined spectrophotometrically, using a Multiskan GO microplate reader (Thermo Fisher Scientific) and normalized to coated monkey IgG standard curves (MyBioSource.com). Neutralizing anti-human FIX Abs were determined by Bethesda assay. The test sample was incubated for 2 hours at 37° C with recombinant human FIX (BENEFIX, Pfizer, 1 U/mL) with FIX activity of 100%. Residual FIX activity was measured using Hyphen Biophen Factor IX kit (Aniara Corp., 221806-RUO) and converted into Bethesda Units (BU)/ml, where one BU is defined as the inverse of the dilution factor of the test sample that yields 50% residual FIX activity.

Statistical analysis

Statistical analyses were performed upon consulting with professional statisticians at the San Raffaele University Center for Statistics in the Biomedical Sciences (CUSSB). When normality assumptions were not met, non-parametric statistical tests were performed. Mann-Whitney or Kruskall-Wallis tests with Dunn's multiple comparison post-test were performed when comparing 2 or more experimental groups, respectively. For repeated measures over time, two-way ANOVA was performed. Comparison between the proportions of IS retrieved in liver and spleen in NHP was performed by the Fisher's exact test. When sample size was <5 and no repeated measurements were available for the same finding, inferential statistical analysis was not performed. In order to test differences in FIX expression or activity over time in NHP, we applied a non-parametric two-way ANOVA (robust rank-based method for factorial designs).

Supplementary Material

Refer to Web version on PubMed Central for supplementary material.

Acknowledgements

We thank A. Nonis, C. Brombin and C. Di Serio of CUSSB for statistical consulting, A. Lombardo and A. Migliara for help with genetic disruption of *CD47*, the ALEMBIC facility at the San Raffaele Scientific Institute for help with electron microscopy analysis, MolMed S.p.A. for large-scale production and purification of the LV batches used in the NHP study, and all members of the Naldini laboratory for helpful discussions. M.M. conducted this study as partial fulfillment of her International Ph.D. Course in Molecular Medicine at San Raffaele University, Milan.

Funding

This work was supported by Telethon (SR-Tiget Core Grant 2011-2016) and Bioverativ sponsored research agreement.

Europe PMC Funders Author Manuscripts

Europe PMC Funders Author Manuscripts

Data and materials availability

The LV and reagents described in this manuscript are available to interested scientists upon signing a MTA with standard provisions. There are some restrictions on use of the provided materials in research involving LV based gene therapy of hemophilia, except for research aimed at reproducing the findings reported in this manuscript, according to the collaboration agreement between F.T., S.R.S.I and Bioverativ. All the data are present in the main text or in the supplementary material.

References

1. Dunbar CE, High KA, Joung JK, Kohn DB, Ozawa K, Sadelain M. Gene therapy comes of age. Science. 2018; 359
2. George LA, Sullivan SK, Giermasz A, Rasko JEJ, Samelson-Jones BJ, Ducore J, Cuker A, Sullivan LM, Majumdar S, Teitel J, McGuinn CE, et al. Hemophilia B Gene Therapy with a High-Specific-Activity Factor IX Variant. The New England journal of medicine. 2017; 377: 2215–2227. [PubMed: 29211678]
3. Nathwani AC, Reiss UM, Tuddenham EG, Rosales C, Chowdary P, McIntosh J, Della Peruta M, Lheriteau E, Patel N, Raj D, Riddell A, et al. Long-term safety and efficacy of factor IX gene therapy in hemophilia B. N Engl J Med. 2014; 371: 1994–2004. [PubMed: 25409372]
4. Rangarajan S, Walsh L, Lester W, Perry D, Madan B, Laffan M, Yu H, Vettermann C, Pierce GF, Wong WY, Pasi KJ. AAV5-Factor VIII Gene Transfer in Severe Hemophilia A. The New England journal of medicine. 2017; 377: 2519–2530. [PubMed: 29224506]
5. High KA, Anguela XM. Adeno-associated viral vectors for the treatment of hemophilia. Hum Mol Genet. 2016; 25 R36-41 [PubMed: 26614390]
6. Naldini L. Gene therapy returns to centre stage. Nature. 2015; 526: 351–360. [PubMed: 26469046]
7. Sessa M, Lorioli L, Fumagalli F, Acquati S, Redaelli D, Baldoli C, Canale S, Lopez ID, Morena F, Calabria A, Fiori R, et al. Lentiviral haemopoietic stem-cell gene therapy in early-onset metachromatic leukodystrophy: an ad-hoc analysis of a non-randomised, open-label, phase 1/2 trial. Lancet. 2016; 388: 476–487. [PubMed: 27289174]
8. Cantore A, Nair N, Della Valle P, Di Matteo M, Matrai J, Sanvito F, Brombin C, Di Serio C, D'Angelo A, Chuah M, Naldini L, et al. Hyperfunctional coagulation factor IX improves the efficacy of gene therapy in hemophilic mice. Blood. 2012; 120: 4517–4520. [PubMed: 23043073]
9. Cantore A, Ranzani M, Bartholomae CC, Volpin M, Valle PD, Sanvito F, Sergi LS, Gallina P, Benedicenti F, Bellinger D, Raymer R, et al. Liver-directed lentiviral gene therapy in a dog model of hemophilia B. Sci Transl Med. 2015; 7 277ra228
10. Brown BD, Venneri MA, Zingale A, Sergi Sergi L, Naldini L. Endogenous microRNA regulation suppresses transgene expression in hematopoietic lineages and enables stable gene transfer. Nat Med. 2006; 12: 585–591. [PubMed: 16633348]
11. Brown BD, Cantore A, Annoni A, Sergi LS, Lombardo A, Della Valle P, D'Angelo A, Naldini L. A microRNA-regulated lentiviral vector mediates stable correction of hemophilia B mice. Blood. 2007; 110: 4144–4152. [PubMed: 17726165]
12. Tao N, Gao GP, Parr M, Johnston J, Baradet T, Wilson JM, Barsoum J, Fawell SE. Sequestration of adenoviral vector by Kupffer cells leads to a nonlinear dose response of transduction in liver. Mol Ther. 2001; 3: 28–35. [PubMed: 11162308]
13. Gordon S. Phagocytosis: An Immunobiologic Process. Immunity. 2016; 44: 463–475. [PubMed: 26982354]
14. Racanelli V, Rehermann B. The liver as an immunological organ. Hepatology. 2006; 43 S54-62 [PubMed: 16447271]
15. Oldenborg PA, Gresham HD, Lindberg FP. CD47-signal regulatory protein alpha (SIRPalpha) regulates Fcgamma and complement receptor-mediated phagocytosis. J Exp Med. 2001; 193: 855–862. [PubMed: 11283158]

Europe PMC Funders Author Manuscripts

16. Takenaka K, Prasolava TK, Wang JC, Mortin-Toth SM, Khalouei S, Gan OI, Dick JE, Danska JS. Polymorphism in Sirpa modulates engraftment of human hematopoietic stem cells. Nat Immunol. 2007; 8: 1313–1323. [PubMed: 17982459]

17. Agudo J, Ruzo A, Kitur K, Sachidanandam R, Blander JM, Brown BD. A TLR and Non-TLR Mediated Innate Response to Lentiviruses Restricts Hepatocyte Entry and Can be Ameliorated by Pharmacological Blockade. Mol Ther. 2012.

18. Oldenborg PA, Zheleznyak A, Fang YF, Lagenaur CF, Gresham HD, Lindberg FP. Role of CD47 as a marker of self on red blood cells. Science. 2000; 288: 2051–2054. [PubMed: 10856220]

19. Majeti R, Chao MP, Alizadeh AA, Pang WW, Jaiswal S, Gibbs KD Jr, van Rooijen N, Weissman IL. CD47 is an adverse prognostic factor and therapeutic antibody target on human acute myeloid leukemia stem cells. Cell. 2009; 138: 286–299. [PubMed: 19632179]

20. Rodriguez PL, Harada T, Christian DA, Pantano DA, Tsai RK, Discher DE. Minimal "Self" peptides that inhibit phagocytic clearance and enhance delivery of nanoparticles. Science. 2013; 339: 971–975. [PubMed: 23430657]

21. Kojima Y, Volkmer JP, McKenna K, Civelek M, Lusis AJ, Miller CL, Direnzo D, Nanda V, Ye J, Connolly AJ, Schadt EE, et al. CD47-blocking antibodies restore phagocytosis and prevent atherosclerosis. Nature. 2016; 536: 86–90. [PubMed: 27437576]

22. Laguette N, Sobhian B, Casartelli N, Ringeard M, Chable-Bessia C, Segeral E, Yatim A, Emiliani S, Schwartz O, Benkirane M. SAMHD1 is the dendritic-and myeloid-cell-specific HIV-1 restriction factor counteracted by Vpx. Nature. 2011; 474: 654–657. [PubMed: 21613998]

23. Escobar G, Moi D, Ranghetti A, Ozkal-Baydin P, Squadrito ML, Kajaste-Rudnitski A, Bondanza A, Gentner B, De Palma M, Mazzieri R, Naldini L. Genetic engineering of hematopoiesis for targeted IFN-alpha delivery inhibits breast cancer progression. Sci Transl Med. 2014; 6 217ra213

24. Milani M, Annoni A, Bartolaccini S, Biffi M, Russo F, Di Tomaso T, Raimondi A, Lengler J, Holmes MC, Scheiflinger F, Lombardo A, et al. Genome editing for scalable production of alloantigen-free lentiviral vectors for in vivo gene therapy. EMBO Mol Med. 2017.

25. Berkowitz RD, Ohagen A, Hoglund S, Goff SP. Retroviral nucleocapsid domains mediate the specific recognition of genomic viral RNAs by chimeric Gag polyproteins during RNA packaging in vivo. J Virol. 1995; 69: 6445–6456. [PubMed: 7666546]

26. Campbell EM, Perez O, Melar M, Hope TJ. Labeling HIV-1 virions with two fluorescent proteins allows identification of virions that have productively entered the target cell. Virology. 2007; 360: 286–293. [PubMed: 17123568]

27. Guidotti LG, Inverso D, Sironi L, Di Lucia P, Fioravanti J, Ganzer L, Fiocchi A, Vacca M, Aiolfi R, Sammicheli S, Mainetti M, et al. Immunosurveillance of the liver by intravascular effector CD8(+) T cells. Cell. 2015; 161: 486–500. [PubMed: 25892224]

28. Benechet AP, Ganzer L, Iannacone M. Intravital Microscopy Analysis of Hepatic T Cell Dynamics. Methods Mol Biol. 2017; 1514: 49–61. [PubMed: 27787791]

29. Huthoff H, Towers GJ. Restriction of retroviral replication by APOBEC3G/F and TRIM5alpha. Trends Microbiol. 2008; 16: 612–619. [PubMed: 18976920]

30. Kimata JT. Stepping toward a macaque model of HIV-1 induced AIDS. Viruses. 2014; 6: 3643–3651. [PubMed: 25256394]

31. Simioni P, Tormene D, Tognin G, Gavasso S, Bulato C, Iacobelli NP, Finn JD, Spiezia L, Radu C, Arruda VR. X-linked thrombophilia with a mutant factor IX (factor IX Padua). N Engl J Med. 2009; 361: 1671–1675. [PubMed: 19846852]

32. Dumont JA, Loveday KS, Light DR, Pierce GF, Jiang H. Evaluation of the toxicology, pharmacokinetics, and local tolerance of recombinant factor IX Fc fusion protein in animals. Thromb Res. 2015; 136: 371–378. [PubMed: 25840744]

33. Nathwani AC, Davidoff AM, Hanawa H, Hu Y, Hoffer FA, Nikanorov A, Slaughter C, Ng CY, Zhou J, Lozier JN, Mandrell TD, et al. Sustained high-level expression of human factor IX (hFIX) after liver-targeted delivery of recombinant adeno-associated virus encoding the hFIX gene in rhesus macaques. Blood. 2002; 100: 1662–1669. [PubMed: 12176886]

34. Biffi A, Bartolomae CC, Cesana D, Cartier N, Aubourg P, Ranzani M, Cesani M, Benedicenti F, Plati T, Rubagotti E, Merella S, et al. Lentiviral vector common integration sites in preclinical

Europe PMC Funders Author Manuscripts

Europe PMC Funders Author Manuscripts

models and a clinical trial reflect a benign integration bias and not oncogenic selection. Blood. 2011; 117: 5332–5339. [PubMed: 21403130]

35. Biffi A, Montini E, Lorioli L, Cesani M, Fumagalli F, Plati T, Baldoli C, Martino S, Calabria A, Canale S, Benedicenti F, et al. Lentiviral hematopoietic stem cell gene therapy benefits metachromatic leukodystrophy. Science. 2013; 341 1233158 [PubMed: 23845948]
36. Aiuti A, Biasco L, Scaramuzza S, Ferrua F, Cicalese MP, Baricordi C, Dionisio F, Calabria A, Giannelli S, Castiello MC, Bosticardo M, et al. Lentiviral hematopoietic stem cell gene therapy in patients with Wiskott-Aldrich syndrome. Science. 2013; 341 1233151 [PubMed: 23845947]
37. Hughes R, Towers G, Noursadeghi M. Innate immune interferon responses to human immunodeficiency virus-1 infection. Rev Med Virol. 2012; 22: 257–266. [PubMed: 22359246]
38. Finkelshtein D, Werman A, Novick D, Barak S, Rubinstein M. LDL receptor and its family members serve as the cellular receptors for vesicular stomatitis virus. Proc Natl Acad Sci U S A. 2013; 110: 7306–7311. [PubMed: 23589850]
39. Annoni A, Brown BD, Cantore A, Sergi LS, Naldini L, Roncarolo MG. In vivo delivery of a microRNA-regulated transgene induces antigen-specific regulatory T cells and promotes immunologic tolerance. Blood. 2009; 114: 5152–5161. [PubMed: 19794140]
40. Brown BD, Gentner B, Cantore A, Colleoni S, Amendola M, Zingale A, Baccarini A, Lazzari G, Galli C, Naldini L. Endogenous microRNA can be broadly exploited to regulate transgene expression according to tissue, lineage and differentiation state. Nat Biotechnol. 2007; 25: 1457–1467. [PubMed: 18026085]
41. Sosale NG, Ivanovska II, Tsai RK, Swift J, Hsu JW, Alvey CM, Zoltick PW, Discher DE. “Marker of Self” CD47 on lentiviral vectors decreases macrophage-mediated clearance and increases delivery to SIRPA-expressing lung carcinoma tumors. Mol Ther Methods Clin Dev. 2016; 3 16080 [PubMed: 28053997]
42. Jacobs F, Wisse E, De Geest B. The role of liver sinusoidal cells in hepatocyte-directed gene transfer. Am J Pathol. 2010; 176: 14–21. [PubMed: 19948827]
43. Mingozzi F, Hasbrouck NC, Basner-Tschakarjan E, Edmonson SA, Hui DJ, Sabatino DE, Zhou S, Wright JF, Jiang H, Pierce GF, Arruda VR, et al. Modulation of tolerance to the transgene product in a nonhuman primate model of AAV-mediated gene transfer to liver. Blood. 2007; 110: 2334–2341. [PubMed: 17609423]
44. Montini E, Cesana D, Schmidt M, Sanvito F, Bartholomae CC, Ranzani M, Benedicenti F, Sergi LS, Ambrosi A, Ponzoni M, Doglioni C, et al. The genotoxic potential of retroviral vectors is strongly modulated by vector design and integration site selection in a mouse model of HSC gene therapy. J Clin Invest. 2009; 119: 964–975. [PubMed: 19307726]
45. Wang L, Zoppe M, Hackeng TM, Griffin JH, Lee KF, Verma IM. A factor IX-deficient mouse model for hemophilia B gene therapy. Proc Natl Acad Sci U S A. 1997; 94: 11563–11566. [PubMed: 9326649]
46. Amabile A, Migliara A, Capasso P, Biffi M, Cittaro D, Naldini L, Lombardo A. Inheritable Silencing of Endogenous Genes by Hit-and-Run Targeted Epigenetic Editing. Cell. 2016; 167: 219–232. e214 [PubMed: 27662090]
47. Lombardo A, Cesana D, Genovese P, Di Stefano B, Provasi E, Colombo DF, Neri M, Magnani Z, Cantore A, Lo Riso P, Damo M, et al. Site-specific integration and tailoring of cassette design for sustainable gene transfer. Nat Methods. 2011; 8: 861–869. [PubMed: 21857672]
48. Matrai J, Cantore A, Bartholomae CC, Annoni A, Wang W, Acosta-Sanchez A, Samara-Kuko E, De Waele L, Ma L, Genovese P, Damo M, et al. Hepatocyte-targeted expression by integrase-defective lentiviral vectors induces antigen-specific tolerance in mice with low genotoxic risk. Hepatology. 2011; 53: 1696–1707. [PubMed: 21520180]
49. Firouzi S, Lopez Y, Suzuki Y, Nakai K, Sugano S, Yamochi T, Watanabe T. Development and validation of a new high-throughput method to investigate the clonality of HTLV-1-infected cells based on provirus integration sites. Genome Med. 2014; 6: 46. [PubMed: 25028597]
50. Gillet NA, Malani N, Melamed A, Gormley N, Carter R, Bentley D, Berry C, Bushman FD, Taylor GP, Bangham CR. The host genomic environment of the provirus determines the abundance of HTLV-1-infected T-cell clones. Blood. 2011; 117: 3113–3122. [PubMed: 21228324]

51. Spinozzi G, Calabria A, Brasca S, Beretta S, Merelli I, Milanesi L, Montini E. VISPA2: a scalable pipeline for high-throughput identification and annotation of vector integration sites. BMC Bioinformatics. 2017; 18: 520. [PubMed: 29178837]

52. Abel U, Deichmann A, Nowrouzi A, Gabriel R, Bartholomae CC, Glimm H, von Kalle C, Schmidt M. Analyzing the number of common integration sites of viral vectors--new methods and computer programs. PLoS One. 2011; 6 e24247 [PubMed: 22022353]

53. Cesana D, Ranzani M, Volpin M, Bartholomae C, Duros C, Artus A, Merella S, Benedicenti F, Sergi Sergi L, Sanvito F, Brombin C, et al. Uncovering and dissecting the genotoxicity of self-inactivating lentiviral vectors in vivo. Mol Ther. 2014; 22: 774–785. [PubMed: 24441399]

Europe PMC Funders Author Manuscripts

Europe PMC Funders Author Manuscripts

Europe PMC Funders Author Manuscripts

Europe PMC Funders Author Manuscripts

One Sentence Summary

Lentiviral vectors with high surface content of CD47 improved gene transfer efficiency to hepatocytes in non-human primates.

Europe PMC Funders Author Manuscripts

Europe PMC Funders Author Manuscripts

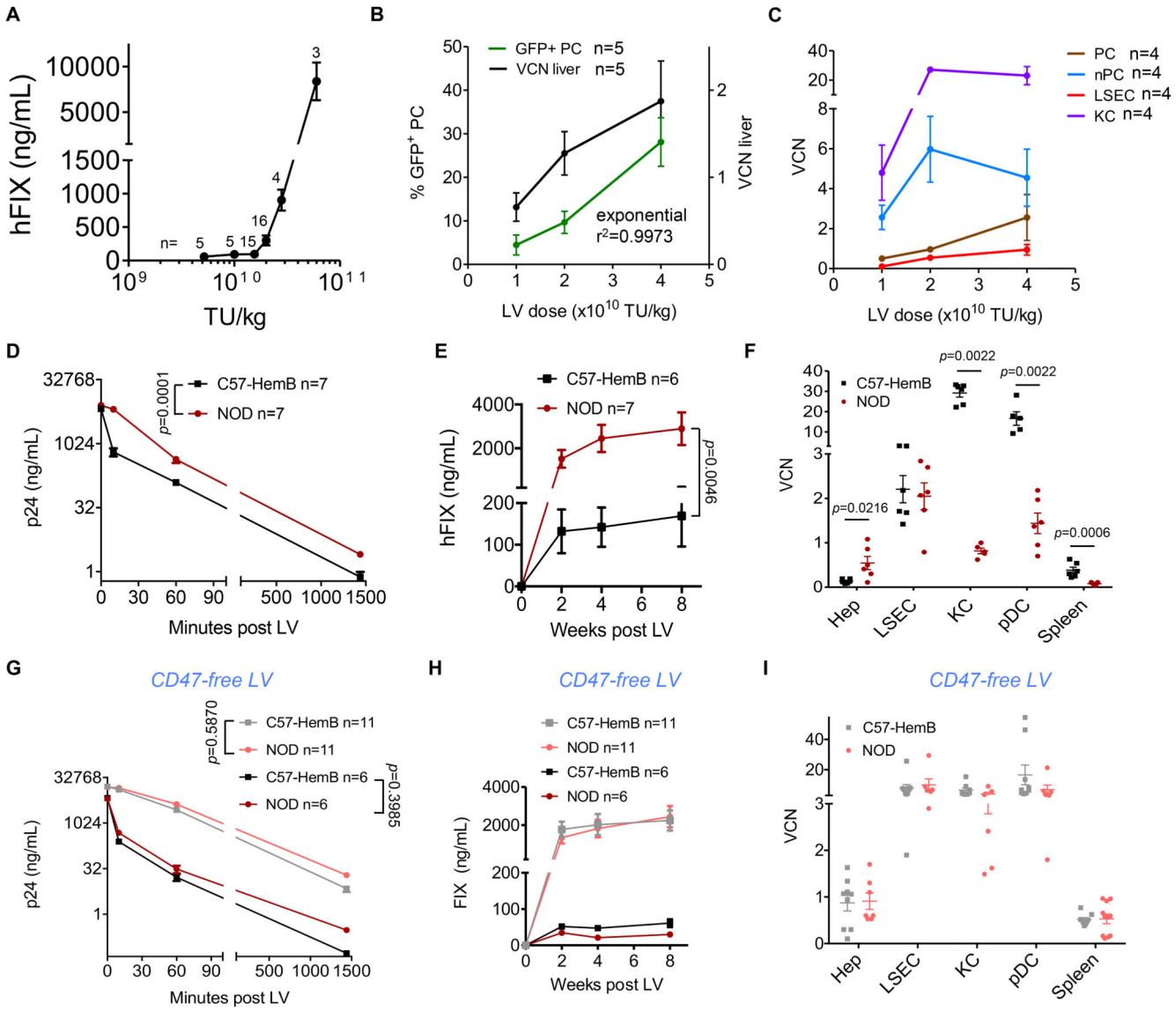

Fig. 1. Role of CD47 in LV biodistribution within the liver of i.v. injected mice.

(**A**) Mean with standard error of the mean (SEM) of human FIX (hFIX) expression measured in the plasma of C57BL/6 mice treated at the indicated LV doses (n=48, from 8 independent experiments, performed with 3 different LV batches; the n of mice per dose is reported on the top of each point). (**B**) Mean with SEM of percentage of GFP-positive PC (green line) in liver sections (5-10 optical fields scored from 6-8 non-consecutive sections/ mouse), and VCN measured in genomic DNA extracted from whole liver (black line), of mice treated with the indicated dose of LV with hepatocyte-specific expression, 2 months after administration (n=5 per dose cohort). (**C**) Mean with SEM of VCN measured in fractionated liver PC (brown line) or nPC (light blue line), FACS-sorted LSEC (red line) or KC (purple line) of mice 2 months after LV administration (n=4 per dose cohort). (**D,E**) Mean with SEM of (D) LV particles (ng HIV Gag p24/mL) measured in serum, and (E) human FIX expression (ng/mL) measured in plasma of C57BL/6 hemophilia B mice (n=6,

Europe PMC Funders Author Manuscripts

Europe PMC Funders Author Manuscripts

black line) or NOD mice (n=6, dark red line), treated with LV-FIX at the indicated time after administration. Two-way ANOVA for repeated measures. (**F**) Single values and mean with SEM of VCN measured in FACS-sorted hepatocytes (Hep), LSEC, KC or pDC, and whole spleen, as indicated, of C57BL/6 hemophilia B mice (n=5-6, black circles) or NOD mice (n=5-6, dark red circles), 2 months after administration ($1.2x10^{10}$ TU/kg). Mann-Whitney test. (**G,H**) Mean with SEM of (G) LV particles or (H) human FIX expression as in (D,E) measured in C57BL/6 hemophilia B mice or NOD mice, treated with LV-FIX produced by CD47-negative 293T cells at $1.2x10^{10}$ TU/kg (C57-HemB n=11 black line; NOD n=11 dark red line) or $2x10^{10}$ TU/kg (C57-HemB n=6 grey line; NOD n=6 pink line). Two-way ANOVA for repeated measures. (**I**) Single values and mean with SEM of VCN measured as in (F), of C57BL/6 hemophilia B mice (n=9) or NOD mice (n=7-11), 2 months after CD47free LV administration ($2x10^{10}$ TU/kg). Mann-Whitney test.

Europe PMC Funders Author Manuscripts

Europe PMC Funders Author Manuscripts

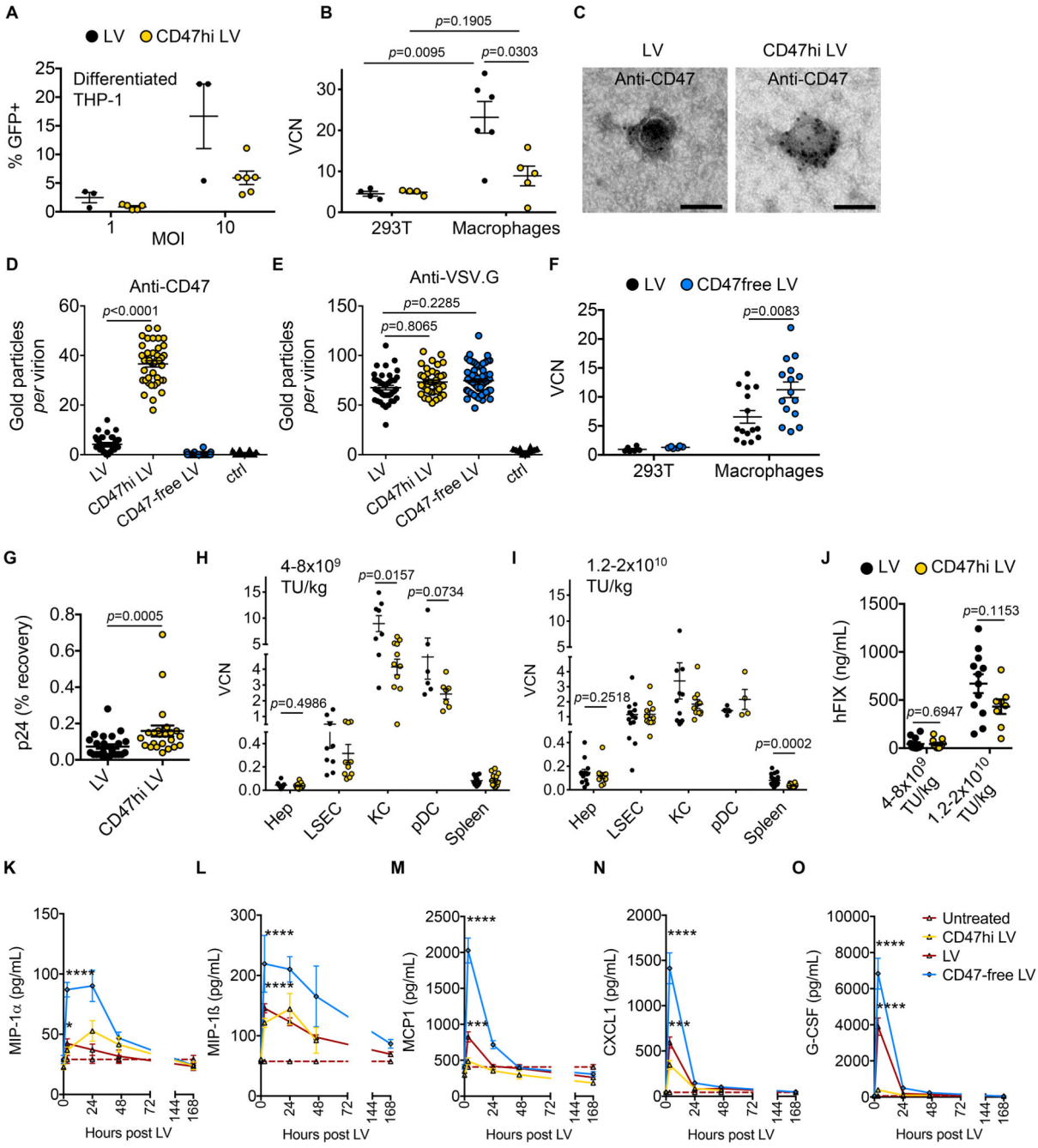

Fig. 2. Generation and evaluation of CD47hi LV.

(**A**) Single values and mean with SEM of percentage of GFP-positive differentiated THP-1 cells transduced with LV (n=3, black circles) or CD47hi LV (n=6, yellow circles), at the indicated multiplicity of infection (MOI) analyzed by flow cytometry, 3 days after transduction (2 independent experiments performed with 2 different CD47hi LV batches). (**B**) Single values and mean with SEM of VCN in 293T cells and primary human macrophages transduced with LV (n=4 for 293T, n=6 for macrophages) or CD47hi LV (n=4 for 293T, n=5 for macrophages) at MOI 10 and analyzed 3 days after transduction

Europe PMC Funders Author Manuscripts

Europe PMC Funders Author Manuscripts

(2 independent experiments performed with 2 different CD47hi LV batches produced by transfection into CD47-overexpressing 293T cells or by CD47-overexpressing LV-GFP stable producer cell line and 2 different healthy blood donors). Mann-Whitney test. (**C-E**) Representative photomicrographs (C) and quantitative analysis (D,E) of LV batches produced by control (LV, black circles), CD47-overexpressing (CD47hi LV, yellow circles), or CD47-negative 293T cells (CD47-free LV, light blue circles), immunostained with anti-CD47 (D) or anti-VSV.G **(E)** antibodies, as indicated, or as staining control without the primary antibody (ctrl, black triangles) and analyzed by electron microscopy (n=41-70 virions per sample). Kruskal-Wallis test with Dunn's multiple comparison test. Bar, 100 nm. (**F**) Single values and mean with SEM of VCN in 293T cells and primary human macrophages (n=6 for 293T, n=15 for macrophages) transduced with LV (black circles) or CD47-free LV (light blue circles) at MOI 10 and analyzed 3 days after transduction (2 independent experiments with 5 different healthy blood donors). Mann-Whitney test. Note that VCN denotes integrated or non-integrated reverse-transcribed LV genome. (**G**) Single values and mean with SEM of percentage of HIV Gag p24 recovered at 24 hours compared to 10 minutes after LV (n=25, black circles) or CD47hi LV (n=23, yellow circles) administration to NOD mice. Mann-Whitney test. (**H,I**) Single values and mean with SEM of VCN in FACS-sorted hepatocytes (Hep), LSEC, KC or pDC, and whole spleen, as indicated, of NOD mice **(H)** injected with LV (n=13-19, n=4 for pDC, black circles) or CD47hi LV (n=11-16, n=4 for pDC, yellow circles) at 1.2-2x10^{10} TU/kg (3 independent experiments) or **(I)** injected with LV (n=6-12) or CD47hi LV (n=7-14) at 4-8x10^{9} TU/kg (3 independent experiments). VCN measured 2 months after LV administration. Mann-Whitney test. (**J**) Single values and mean with SEM of human FIX expression (ng/mL) measured in plasma of NOD mice injected with LV (n=12) or CD47hi LV (n=8-11) at the indicated vector dose. Mann-Whitney test. (**K-O**) Mean with SEM of the concentration of **(K)** MIP-1α, **(L)** MIP-1β, **(M)** MCP1, **(N)** CXCL1 and **(O)** G-CSF in the serum of NOD mice at the indicated time after administration of LV (n=29 for K-M; n=14 for N,O), CD47hi LV (n=12 for K-M; n=7 for N,O), CD47-free LV (n=11 for K-M; n=7 for N,O) or left untreated (n=17 for K-M; n=12 for N,O). The dashed lines show the mean concentration in untreated cohorts. Kruskal-Wallis test with Dunn's multiple comparison test. Reported statistics refer to comparison between LV- (red line) or CD47free-LV (blue line) treated and untreated (dashed line) mice 3 hours post LV administration. $p<0.05$ = *; $p<0.01$ = **; $p<0.001$ = ***; $p<0.0001$ = ****. Complete statistical analysis of data in (K-O) is in Fig. S5.

Europe PMC Funders Author Manuscripts

Europe PMC Funders Author Manuscripts

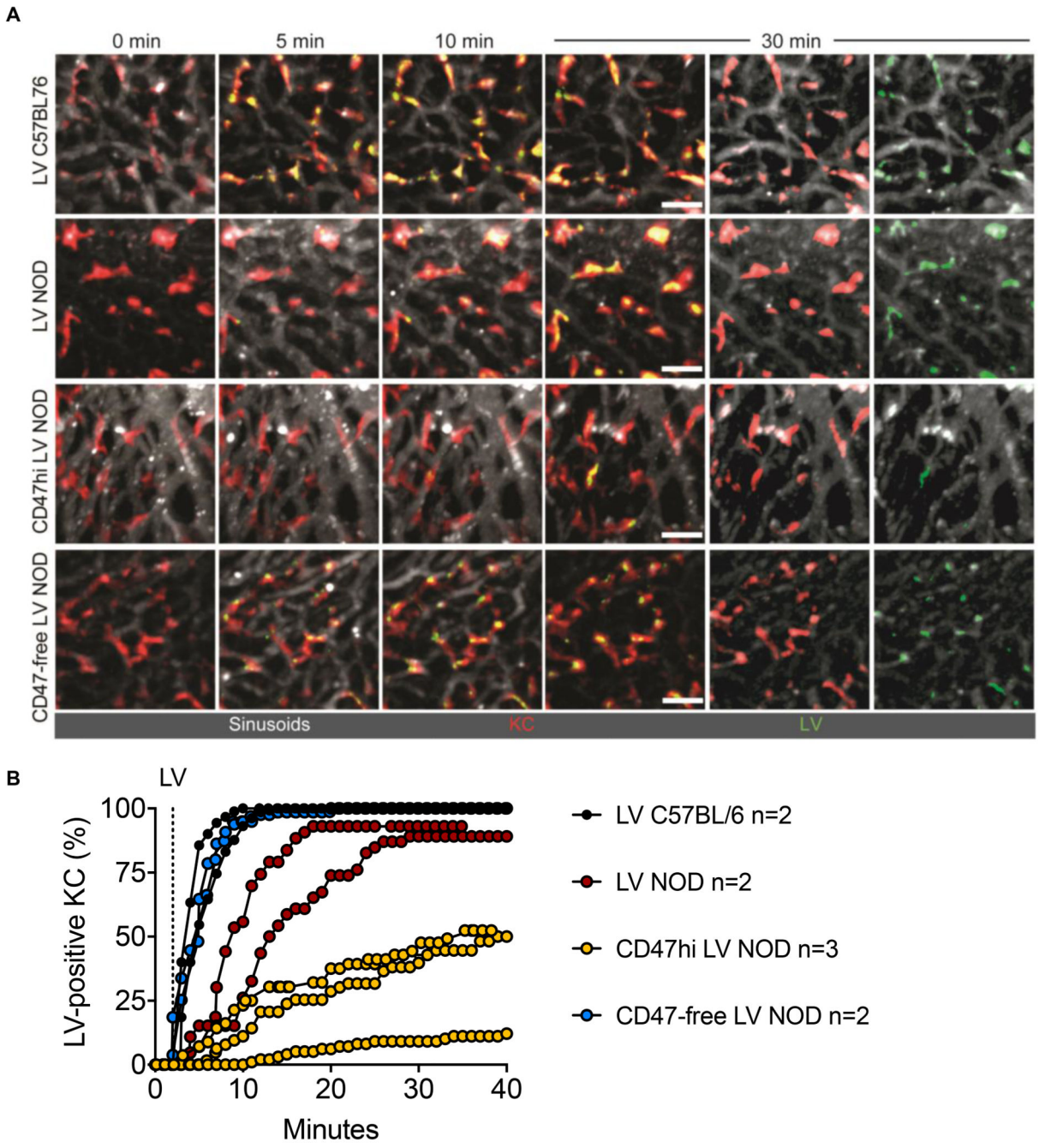

Fig. 3. Intravital imaging of LV, CD47hi or CD47-free LV uptake by liver KC in mice.

(**A**) IV2PM images from 8–12 z-stacks spacing 4 μm of liver of C57BL/6 or NOD mice treated with GFP-labeled LV, CD47hi or CD47-free LV as indicated, at the indicated time (minutes; note that LV i.v. injection starts at min 2). Sinusoids are labeled in white, KC in red. Scale bar, 30 μm. Separate channels (white and red or white and green) are also shown for the 30-min time point. (**B**) Single values of the percentage of LV-positive KC (yellow stained) over time in C57BL/6 or NOD mice treated with LV, CD47hi or CD47-free LV, as indicated (analyzed KC *per* mouse n = 43-130).

Europe PMC Funders Author Manuscripts

Europe PMC Funders Author Manuscripts

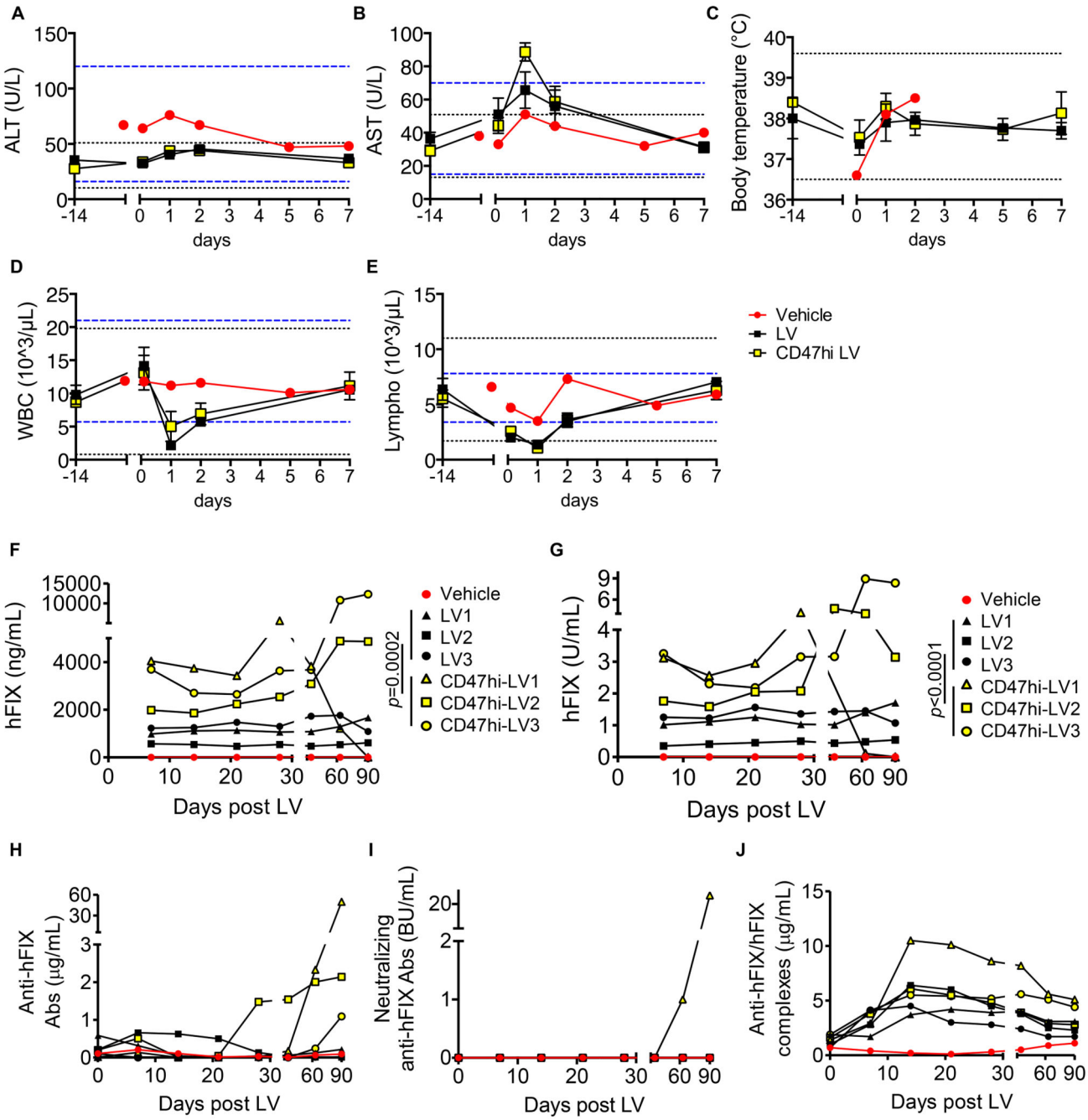

Fig. 4. Tolerability and efficacy of i.v. LV gene therapy in NHP.

(**A-E**) Mean with SEM of the concentration of (A) ALT, (B) AST, (C) body temperature, (D) counts of WBC and (E) lymphocytes of vehicle (n=1, red circles), LV-treated (n=3, black squares) or CD47hi-LV treated NHP (n=3, yellow squares) at the indicated time after administration. The black dashed lines show the mean±3SD calculated on 14 pre-LV samples taken from the same animals; the blue dashed lines show the normal reference values for *Macaca fascicularis*. (**F-J**) Concentration of (F) human FIX antigen or (G) human FIX activity measured in the plasma, or (H) total anti-human FIX Abs, or (I) neutralizing

anti-human FIX Abs, or (J) anti-human FIX/human FIX immune complexes measured in the serum of vehicle (n=1, red circles), LV-treated (n=3, black symbols) or CD47hi-LV treated NHP (n=3, yellow symbols) at the indicated time after administration; U: units; BU: Bethesda Units. Non-parametric two-way ANOVA on the first 30 days post LV.

Europe PMC Funders Author Manuscripts

Europe PMC Funders Author Manuscripts

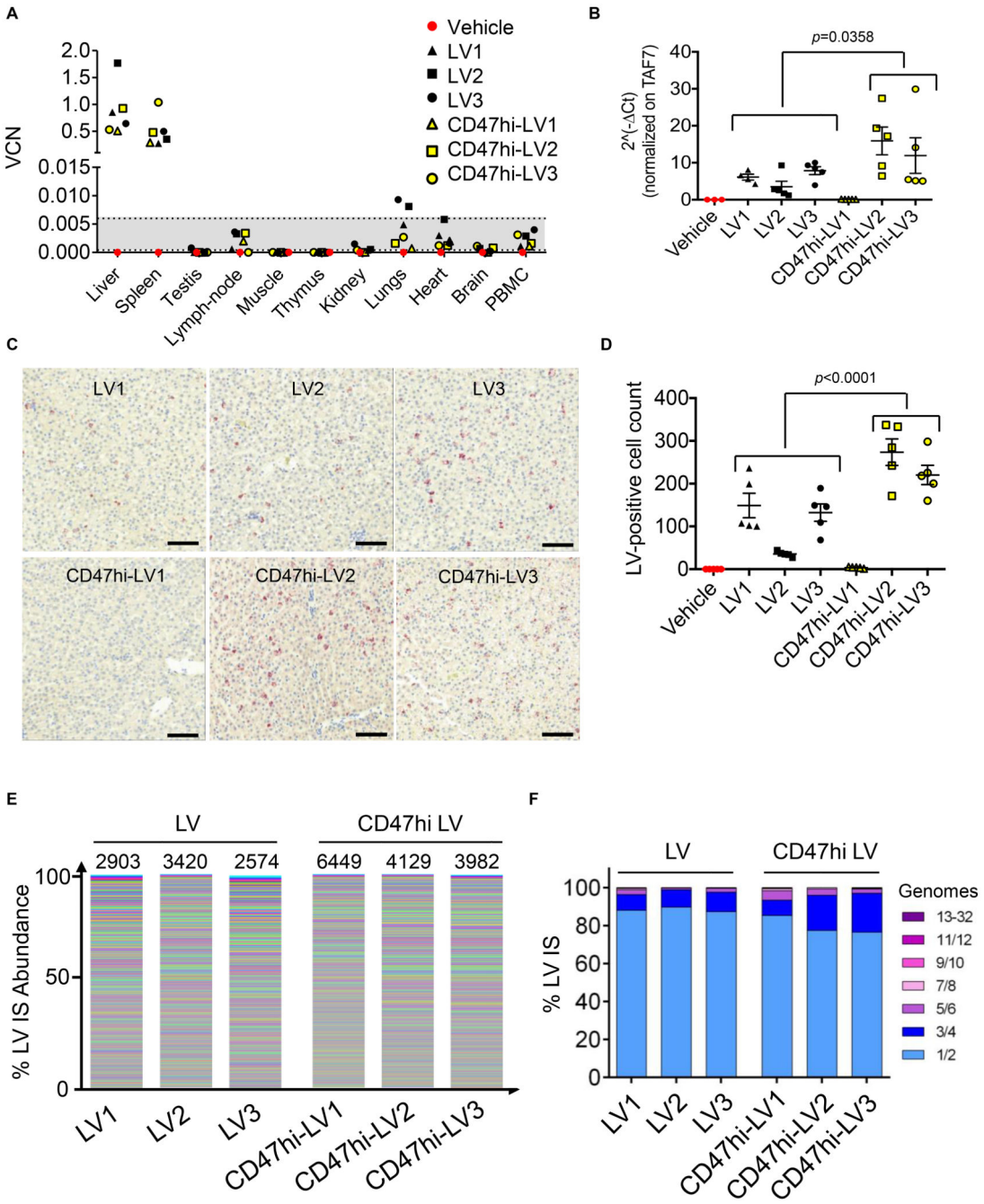

Fig. 5. Selectivity of i.v. LV gene therapy in NHP and IS analysis.

(**A**) Single values of VCN in the indicated organs of vehicle-, LV- or CD47hi-LV treated NHP at necropsy (90 days post LV). The dashed lines defining the grey area represent the lower limit of detection (0.0004) and the lower limit of quantification (0.006), thus values in the grey area can be detected (different from the negative control), but not reliably quantified (see methods section). (**B**) Expression analysis by qRT-PCR of WPRE normalized on the endogenous TAF7 gene ($2^{\wedge}$-ΔCt) on RNA extracted from different liver lobes of LV- or CD47hi-LV treated NHP, as indicated. Mann-Whitney test. (**C,D**) Counts of LV-RNA

Europe PMC Funders Author Manuscripts
Europe PMC Funders Author Manuscripts

positive cells (D, LV-expressing cells) by ISH on liver tissue slices of the indicated NHP (n=5 random fields taken from 5 non-consecutive slides/NHP); representative images are shown in (C). Scale bar 100 μm. Mann-Whitney test. (**E,F**) Stacked bar plots representing the abundance of each LV IS retrieved from the liver of LV- or CD47hi-LV treated NHP. In (E) each LV IS is represented by a different color with the height in relative proportion with the number of retrieved genomes (frequency) over the total. In (F) the frequency by which individual LV integrations are found in 1 or more genomes are plotted in groups of increasing number of genomes.

Europe PMC Funders Author Manuscripts

Europe PMC Funders Author Manuscripts